Neuropharmacology 138 (2018) 371–380

Contents lists available at ScienceDirect

Neuropharmacology

journal homepage: www.elsevier.com/locate/neuropharm

Attenuated dopaminergic neurodegeneration and motor dysfunction in hemiparkinsonian mice lacking the α5 nicotinic acetylcholine receptor subunit

Sakari Leino, Sini K. Koski, Raisa Hänninen, Tuukka Tapanainen, Saara Rannanpää, Outi Salminen*

Division of Pharmacology and Pharmacotherapy, Faculty of Pharmacy, University of Helsinki, 00014 Helsinki, Finland

ARTICLE INFO

Article history:
Received 4 December 2017
Received in revised form
4 June 2018
Accepted 21 June 2018
Available online 22 June 2018

Keywords:
Parkinson's disease
Nicotinic receptors
Chrna5 subunit
Levodopa-induced dyskinesia
Substantia nigra
Dopamine

ABSTRACT

Preclinical studies suggest the involvement of various subtypes of nicotinic acetylcholine receptors in the pathophysiology of Parkinson's disease, a neurodegenerative disorder characterized by the death of dopaminergic neurons in the substantia nigra pars compacta (SNC). We studied for the first time the effects of α5 nicotinic receptor subunit gene deletion on motor behavior and neurodegeneration in mouse models of Parkinson's disease and levodopa-induced dyskinesia. Unilateral dopaminergic lesions were induced in wild-type and α5-KO mice by 6-hydroxydopamine injections into the striatum or the medial forebrain bundle. Subsequently, rotational behavior induced by dopaminergic drugs was measured. A subset of animals received chronic treatments with levodopa and nicotine to assess levodopa-induced dyskinesia and antidyskinetic effects by nicotine. SNC lesion extent was assessed with tyrosine hydroxylase immunohistochemistry and stereological cell counting. Effects of α5 gene deletion on the dopaminergic system were investigated by measuring *ex vivo* striatal dopamine transporter function and protein expression, dopamine and metabolite tissue concentrations and dopamine receptor mRNA expression. Hemiparkinsonian α5-KO mice exhibited attenuated rotational behavior after amphetamine injection and attenuated levodopa-induced dyskinesia. In the intrastriatal lesion model, dopaminergic cell loss in the medial cluster of the SNC was less severe in α5-KO mice. Decreased striatal dopamine uptake in α5-KO animals suggested reduced dopamine transporter function as a mechanism of attenuated neurotoxicity. Nicotine reduced dyskinesia severity in wild-type but not α5-KO mice. The attenuated dopaminergic neurodegeneration and motor dysfunction observed in hemiparkinsonian α5-KO mice suggests potential for α5 subunit-containing nicotinic receptors as a novel target in the treatment of Parkinson's disease.

1. Introduction

Parkinson's disease is a neurodegenerative disorder characterized by the death of dopaminergic neurons in the substantia nigra pars compacta (SNC), a deficit of dopamine in the dorsal striatum, and resulting motor deficits (Dauer and Przedborski, 2003). No treatment affecting the disease progression is available. Dopamine replacement therapy with levodopa (L-3,4-dihydroxyphenylalanine) is effective for symptomatic relief, but often complicated by abnormal involuntary movements (levodopa-induced dyskinesia, LID) after long-term treatment (Bastide et al., 2015; Schapira et al., 2009).

Neuronal nicotinic acetylcholine receptors are ion channel receptors composed of five subunits (α2–α10, β2–β4), with the homomeric α7 receptor and the heteromeric α4β2* receptor (asterisk denoting the possible presence of other subunits) being the most widely expressed (Albuquerque et al., 2009; Millar and Gotti, 2009). Through nicotinic receptors, the brain cholinergic

Abbreviations: 6-OHDA, 6-hydroxydopamine; DAT, dopamine transporter; DOPAC, 3,4-dihydroxyphenylacetic acid; HVA, homovanillic acid; LID, levodopa-induced dyskinesia; MFB, medial forebrain bundle; qPCR, quantitative polymerase chain reaction; RM-ANOVA, repeated measures analysis of variance; SNC, substantia nigra pars compacta; SNCD, dorsal tier of the SNC; SNCM, medial cluster of the SNC; TH, tyrosine hydroxylase.

* Corresponding author. Faculty of Pharmacy, P.O. Box 56, 00014, University of Helsinki, Finland.
E-mail address: outi.salminen@helsinki.fi (O. Salminen).

https://doi.org/10.1016/j.neuropharm.2018.06.028

system modulates the activity of other neurotransmitter systems, including the nigrostriatal dopaminergic pathway essential for motor control that is degenerated in Parkinson's disease (Livingstone and Wonnacott, 2009; Quik and Wonnacott, 2011).

The α5 nicotinic receptor subunit is an accessory subunit that can form a heteromeric receptor in combination with α4 and β2 subunits (Kuryatov et al., 2008). The α5 subunit does not contribute to ligand binding, but α5 incorporation results in changes in receptor function such as increased calcium permeability (Tapia et al., 2007) and lessened propensity for desensitization (Grady et al., 2012). Mice lacking the α5 subunit show impaired attention, increased anxiety, and decreased novelty-induced behavior as well as a decreased sensitivity to nicotine (Bailey et al., 2010; Besson et al., 2016; Jackson et al., 2010). Findings such as these suggest a key role for α5* receptors in a number of behavioral functions and illustrate their potential as a treatment target for various neurological and psychiatric disorders.

In the case of Parkinson's disease, several paths of evidence point to a role for nicotinic receptors in the pathophysiology and treatment of the disease; for a recent review, see Quik et al. (2015). In brief, epidemiological studies show that the use of tobacco products can be protective against the disease, and nicotinic agonists can be neuroprotective in animal models of dopaminergic neurodegeneration. Nicotinic agonists have also been shown to alleviate LID in multiple animal models. Results obtained with selective ligands and subunit-null mice suggest that the neuroprotective effects are mediated by at least α4* and α7 nicotinic receptors (Bordia et al., 2015; Ryan et al., 2001), and that α4β2*, α6β2* and α7 nicotinic receptors all influence the expression of LID (Quik et al., 2013).

A significant role in Parkinson's disease might also be expected for α5* nicotinic receptors, considering their major contribution to the presynaptic regulation of nigrostriatal dopamine release in the dorsal striatum (Exley et al., 2012; Salminen et al., 2004). The potential consequences of α5* intervention in Parkinson's disease have, however, not been studied before. Therefore, we studied here the effects of genetic deletion of the α5 subunit in mouse models of Parkinson's disease and LID. We found that the lack of α5* nicotinic receptors resulted in attenuated dopaminergic pathophysiology, suggesting their potential as a novel target in the treatment of Parkinson's disease.

2. Materials and methods

2.1. Animals

α5-knockout (α5-KO) C57BL/6J mice and wild-type (WT) littermates (Salas et al., 2003) were obtained from the Institute for Behavioral Genetics (University of Colorado, Boulder, CO, USA) and bred at the research site. Experiments utilizing striatal lesions and characterizations of intact animals included both sexes. Experiments utilizing medial forebrain bundle (MFB) lesions included only female mice due to penile prolapse complications seen in males after a severe lesion (Thiele et al., 2011). Mice were genotyped as previously described (Salminen et al., 2004) and group housed in a temperature- and humidity-controlled environment under a 12 h light/dark cycle. All experiments were conducted following local and EU laws and regulations and authorized by the national Animal Experiment Board of Finland.

2.2. Drugs

6-hydroxydopamine hydrochloride, apomorphine hydrochloride, benserazide hydrochloride, desipramine hydrochloride, dopamine hydrochloride, levodopa methyl ester hydrochloride, (−)-nicotine, nomifensine maleate and pargyline hydrochloride were from Sigma-Aldrich (St. Louis, MO, USA). Lidocaine was from Orion Pharma (Espoo, Finland), buprenorphine from RB Pharmaceuticals (Berkshire, UK), and carprofen from Pfizer Animal Health (Helsinki, Finland). D-Amphetamine sulphate was synthesized at the Faculty of Pharmacy, University of Helsinki (Finland). [^{3}H] dopamine (58.9 Ci/mmol) was from PerkinElmer (Waltham, MA, USA). Doses of drugs refer to free bases.

2.3. Unilateral 6-OHDA lesion and postoperative care

Unilateral lesioning of the nigrostriatal dopaminergic pathway was induced by stereotactic injection of 6-hydroxydopamine (6-OHDA; in 0.02% ascorbate-saline) under isoflurane anesthesia. Desipramine (25 mg/kg, i.p.) was administered 30 min prior to surgery to inhibit noradrenergic neurodegeneration. Topical lidocaine and systemic buprenorphine (0.1 mg/kg, s.c.) and carprofen (5 mg/kg, s.c.) were used for pain relief. In the intrastriatal model, 6-OHDA was injected into two sites within the left dorsolateral striatum, 6 μg in 1 μl each, at the following coordinates relative to the bregma and the dural surface: A/P +1.0; L/M +1.9; D/V −2.9 and A/P +0.3; L/M +2.0; D/V −2.9. In the intra-MFB model, 6-OHDA (3 μg in 0.2 μl) was injected into the right MFB at the following coordinates: A/P −1.2; L/M −1.1; D/V −5.0. Postoperative care included warm saline injections, heating pads, food pellets softened by soaking, high-energy palatable diet (Bacon Softies, Bio-Serv, Flemington, NJ, USA; Nutriplus gel, Virbac, Carros, France), and feeding by hand. Post-operative mortality was 9% and 14% when utilizing the intrastriatal and intra-MFB lesion models, respectively.

2.4. Measurements of drug-induced locomotor activity

Drug-induced rotation tests were performed 2–3 weeks after the 6-OHDA injections. A Roto-Rat automated rotametry apparatus (Med Associates Inc., St. Albans, VA, USA) was used. Mice were fitted with plastic collars made from cable ties and, after amphetamine (2.5 mg/kg, i.p.) or apomorphine (0.5 mg/kg, i.p.) administration, attached from the collars to automatic detectors with an iron wire and placed in a plexiglass cylinder (11 × 15 cm). Rotations were measured for 90 min (amphetamine) or 40 min (apomorphine) at 5 min intervals and expressed as net ipsi- or contralateral rotations, respectively.

The effect of amphetamine on locomotion of intact mice was measured using an automated infrared activity monitor (Activity Monitor, Med Associates Inc.). Mice were individually placed in a 43 × 43 cm plexiglass chamber for 30 min, after which amphetamine (2.5 mg/kg, i.p.) was administered. The distance travelled by the animal was measured via photobeam interruption during habituation and for 2 h after amphetamine administration.

2.5. Chronic drug treatments and measurement of dyskinesia severity

Female animals lesioned with intra-MFB 6-OHDA injections were administered levodopa (3 mg/kg) and benserazide (15 mg/kg) each weekday (Mon-Fri) in a single s.c. injection. After three weeks, nicotine treatment (up to 300 μg/ml) in saccharin-sweetened drinking water was initiated as previously described (Huang et al., 2011; Pietilä and Ahtee, 2000). Drinking water consumption per cage was measured every 3–4 days. Treatment with levodopa and nicotine was continued for 9 weeks. Dyskinesia severity was assessed from weekly video recordings, where mice were individually recorded for 1 min in transparent cylinders flanked by two vertical mirrors 20, 40, 60, 80 and 100 min after the levodopa

injection. Dyskinesia was classified into axial, orolingual and forelimb dyskinesia and rated on a scale of 0–4 according to previously described criteria (Leino et al., 2018). A weekly score was calculated as the sum of rating scores from each subtype and time point.

2.6. Immunohistochemistry and stereological cell counting

Mice were killed by cervical dislocation and the posterior part of the brain was immersed overnight in 4% paraformaldehyde in PBS at +4 °C and stored in 20% sucrose in PBS at +4 °C until freezing in isopentane on dry ice. Free-floating coronal sections of 40 μm (intrastriatal model) or 30 μm (intra-MFB model) thickness were cut with a Leica CM3050 cryostat (Leica Biosystems, Wetzlar, Germany). Sections were immunostained for tyrosine hydroxylase (TH) essentially as described by Mijatovic et al. (2007), with the exception that data from the intrastriatal model were obtained using biotinylated protein A (prepared using protein A [MP Biomedicals, Santa Ana, CA, USA] and N-hydroxysuccinimido-biotin [Sigma-Aldrich]) in place of the secondary antibody.

The number of TH-positive neurons in the dorsal tier (SNCD) and the medial cluster (SNCM) of the SNC were estimated by blinded unbiased stereological cell counting. Demarcation of brain areas followed published delineations (Franklin and Paxinos, 1997; Fu et al., 2012). Three consequent sections (every third section for intrastriatally lesioned animals, every sixth section in intra-MFB lesioned animals) were selected between levels −2.9 and −3.4 mm from the bregma for SNCD and between −3.1 and −3.6 mm for SNCM. StereoInvestigator (MBF Bioscience, Williston, VT, USA) was used to first outline the region at 4x magnification and then count stained cell bodies with an optical fractionator, according to optical disector rules (Gundersen et al., 1988), at regular intervals (SNCD: x = 80 μm, y = 80 μm; SNCM: x = 60 μm, y = 60 μm) within a counting frame (60 μm × 60 μm) superimposed on an image obtained using a 60x oil objective (Olympus Plan/Apo, Olympus, Tokyo, Japan). Gundersen's coefficients of error (CE) were ≤0.15 for the intact hemisphere. Data were expressed as percentage of the intact hemisphere.

2.7. Dopamine uptake assay

Preparation of P2 synaptosomal pellets from fresh striatal tissue and resuspension in uptake buffer were performed as previously described (Salminen et al., 2004), with the following exceptions: tissue was homogenized in a volume of 2 ml and a 0.2 ml aliquot taken for centrifugation; uptake buffer additionally contained 0.1% bovine serum albumin. The uptake assay was performed in a MultiScreen HTS 96-well filter-bottomed plate (Millipore, Bedford, MA, USA) in a volume of 100 μl uptake buffer containing 25 μl of the synaptosome suspension and 1 μM dopamine (2% [^{3}H]dopamine). 200 μM nomifensine was used for blank determination. Solutions were incubated for 30 min in room temperature before aspiration and washing the filters with 6 × 200 μl cold uptake buffer. Super-Mix scintillation cocktail (100 μl/well; PerkinElmer) was added, and radioactivity measured with liquid scintillation counting (5 min per well; 1450 MicroBeta TriLux; Wallac, Turku, Finland). The protein concentrations of synaptosomal suspensions were measured using the Bradford method (Bradford Reagent, Sigma-Aldrich). Data were expressed as pmol of dopamine taken up per μg of protein.

2.8. Western blotting

Dopamine transporter (DAT), phospho (T53)-DAT (pDAT) and β-actin protein levels in striatal tissue samples from intact mice were measured with Western blotting. Sample preparation from frozen tissue and Western blotting were performed using the methods and antibodies described by Julku et al. (2018), with the following exceptions: 4–20% (DAT) and 8–16% (pDAT) Mini-PROTEAN TGX precast gels (Bio-Rad, Hercules, CA, USA) were used; a different rabbit anti-β-actin antibody (#ab8227, AbCam, Cambridge, UK; diluted 1:2000) was used; all antibodies were diluted in 5% skim milk in 0.05% Tween-20 in tris-buffered saline; all blots were performed by incubating the membrane with the primary antibody overnight at +4 °C and subsequently with the secondary antibody for 2 h at room temperature. Optical density values were normalized to loading control (β-actin) optical density values, and the data expressed as percentage of wild-type mean.

2.9. High-performance liquid chromatography

Striatal tissue concentrations of dopamine and its metabolites 3,4-dihydroxyphenylacetic acid (DOPAC) and homovanillic acid (HVA) were measured from intact mice using high-performance liquid chromatography (HPLC) as described by Julku et al. (2018). Data were expressed as μg of analyte per gram of wet tissue.

2.10. qPCR

Striatal tissue samples were collected as for HPLC (Julku et al., 2018), frozen with liquid nitrogen and stored at −80 °C. Tissue from age- and sex-matched control mice (C57BL/6) was pooled in two groups to have separate native controls for both hemispheres. RNA was isolated using an RNAeasy Mini kit (Qiagen, Hilden, Germany) and DNase digestion performed using an RNase-Free DNase set (Qiagen) as described by the manufacturer. RNA was quantified with a NanoDrop ND-1000 Spectrophotometer (NanoDrop Technologies, Wilmington, DE, USA) and converted to cDNA by Super-Script III First-Strand Synthesis SuperMix and oligo(dT) primers (Invitrogen, Carlsbad, CA, USA). For qPCR, cDNA was diluted with RNase free water, and 4.5 μl of cDNA used per well in a 10 μl reaction volume. ABsolute Blue QPCR Mix, ROX (Thermo Scientific, Waltham, MA, USA) was mixed with TaqMan primers and hydrolysis probes (Applied Biosystems, Foster City, CA, USA; catalogue numbers: Dopamine 1 receptor, Mm02620146_s1; Dopamine 2 receptor, Mm00438545_m1). PCR amplification was performed on 384-well plates using a Roche LightCycler (Roche Diagnostics, Mannheim, Germany) with 1 cycle of 15 min at 95 °C, 40 cycles of 15 s at 95 °C, and 40 cycles of 1 min at 60 °C by turns. Expression of target genes was normalized to the pooled control with the reference gene GAPDH (TaqMan, Mm99999915_g1). Relative mRNA expression was calculated using the $2^{-\Delta\Delta Ct}$ method and data expressed as fold change in mRNA levels (Livak and Schmittgen, 2001).

2.11. Statistical analysis

Data are expressed as group means ± standard error of the mean (SEM). Statistical analyses were performed with IBM SPSS Statistics 24 (IBM, Armonk, NY, USA). Outliers were removed with the Tukey Box-Plot method (Tukey, 1977). Locomotor data were analyzed with two-way repeated measures analyses of variance (RM-ANOVA; genotype × time); dyskinesia data with three-way RM-ANOVA (genotype × treatment × time); data from immunohistochemistry with two-tailed unpaired t-tests (intra-MFB model) or two-way ANOVA (genotype × sex; intrastriatal model); dopamine uptake, Western blotting and HPLC data with two-way ANOVA (genotype × sex); and qPCR data with three-way ANOVA (genotype × sex × hemisphere). Violations of the assumption of sphericity in RM-ANOVA were corrected for with the Greenhouse-Geisser correction.

3. Results

3.1. Effects of α5 gene deletion in mouse models of Parkinson's disease

Drug-induced locomotion was measured both in unilaterally lesioned hemiparkinsonian animals and in intact animals. In the lesioned animals, the extent of dopaminergic denervation in the dorsal tier (SNCD) and medial cluster (SNCM) of the SNC was determined *post mortem* by stereological cell counting. See Fig. 1 for images of representative brain sections and examples of delineations of the SNCD and the SNCM.

Fig. 2 shows immunohistochemical and behavioral results obtained using the intrastriatal 6-OHDA lesion model. Both subdivisions of the SNC had suffered lesions of roughly similar extent. Numbers of remaining cells were estimated with CE 0.14–0.39 for SNCD and CE 0.12–0.28 for SNCM. In the SNCD, no difference was found between WT and α5-KO animals in TH-positive cells remaining (Fig. 2B; WT 16.6 ± 2.9% vs. α5-KO 18.8 ± 2.9%; main effect of genotype, $F(1,13) = 0.96$, $P = 0.346$). SNCD cell loss tended to be more pronounced in male animals (main effect of sex, $F(1,13) = 4.06$, $P = 0.065$) with no genotype × sex interaction ($F(1,13) = 1.07$, $P = 0.321$). In contrast, in the SNCM more TH-positive cells remained in α5-KO animals when compared to WT animals (Fig. 2C; WT 18.5 ± 2.9% vs. α5-KO 26.9 ± 1.5%; main effect of genotype, $F(1,13) = 6.72$, $P = 0.022$), with similar results for both sexes (males: WT 21.1 ± 3.5% vs. α5-KO 30.0 ± 2.8%; females: WT 17.5 ± 3.9% vs. α5-KO 25.5 ± 1.6%; main effect of sex, $F(1,13) = 1.54$, $P = 0.237$; genotype × sex interaction, $F(1,13) = 0.020$, $P = 0.889$).

As a whole, amphetamine-induced rotational behavior did not significantly differ between α5-KO and WT mice lesioned with intrastriatal 6-OHDA injections ($F(1,18) = 2.12$, $P = 0.162$; data not shown). However, analyzing sexes separately revealed that female α5-KO mice performed fewer ipsilateral rotations than female WT mice (Fig. 2D; $F(1,11) = 5.23$, $P = 0.042$), while among male animals there was no genotype difference in amphetamine-induced rotational behavior (Fig. 2E; $F(1,5) = 0.02$, $P = 0.895$). Among intrastriatally lesioned female mice, α5-KO animals tended to perform fewer apomorphine-induced (0.5 mg/kg) contralateral rotations during the earliest measurement period (Fig. 2F), although the genotype difference was not statistically significant (genotype × time interaction, $F(2.5,27) = 2.40$, $P = 0.100$; main effect of genotype, $F(1,11) < 0.001$, $P = 0.99$). In contrast, male α5-KO mice performed more apomorphine-induced rotations than male WT mice (Fig. 2G; main effect of genotype, $F(1,5) = 16.1$, $P = 0.010$). In intact mice, no genotype difference was observed in the distance travelled after amphetamine (2.5 mg/kg) administration (Fig. 2H; $F(1,25) = 0.01$, $P = 0.930$), with similar results for both sexes (males: $F(1,9) = 0.22$, $P = 0.652$; females: $F(1,14) = 0.39$, $P = 0.544$; data not shown).

The immunohistochemical and behavioral results obtained using the intra-MFB 6-OHDA lesion model are shown in Fig. 3 for females (main experiment) and in supplementary figures for males (pilot experiment). In the main experiment, a severe lesion of the SNCD was readily apparent in all animals, and highly accurate estimates of cell numbers could not be obtained due to only occasional cells remaining. A rough estimate (CE 0.25–0.71) suggested no statistically significant genotype difference in the proportion of TH-positive cells remaining in the lesioned SNCD (Fig. 3B; WT 6.0 ± 0.9% vs. α5-KO 8.5 ± 2.2%, $t(15) = 1.02$, $P = 0.323$). In the SNCM, a much less severe lesion was apparent, and more accurate estimates could be obtained (CE 0.13–0.24). No significant genotype difference was found in the proportion of TH-positive cells remaining in the lesioned SNCM (Fig. 3C; WT 45.1 ± 5.2% vs. α5-KO 36.4 ± 3.7%, $t(15) = 1.41$, $P = 0.180$). Striatal denervation was characterized in the pilot experiment, where fewer severe striatal lesions were observed in α5-KO than in wild-type animals (Figure S1).

Female α5-KO mice of the intra-MFB model tended to perform fewer amphetamine-induced (2.5 mg/kg) ipsilateral rotations than

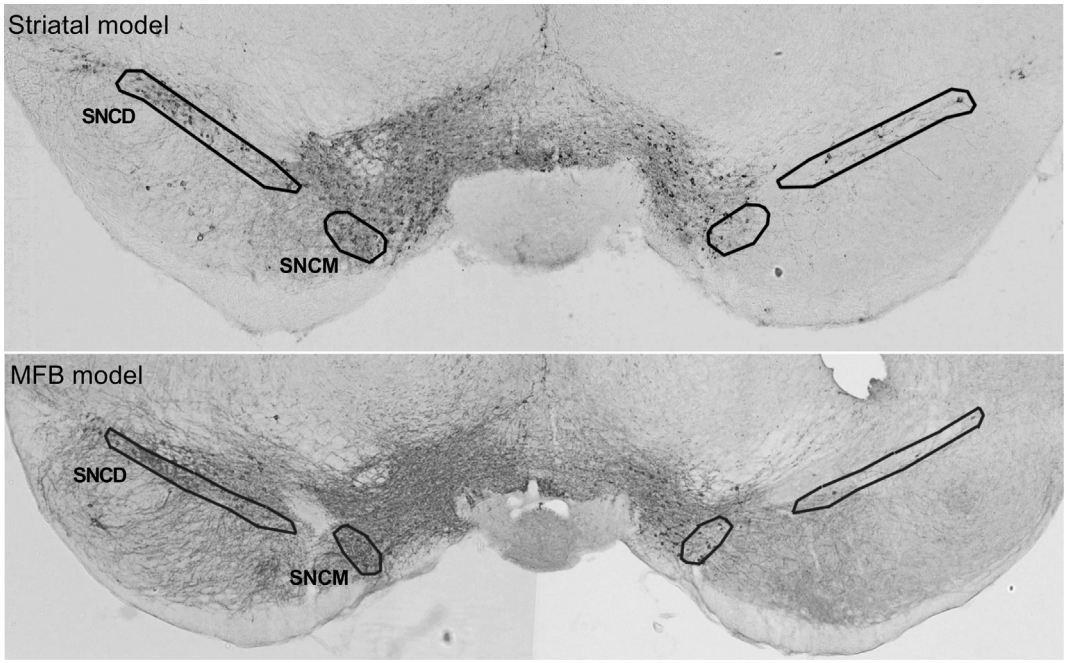

Fig. 1. Tyrosine hydroxylase immunohistochemistry and the brain areas studied. The figure shows representative sections from two animals (top: intrastriatal model; bottom: intra-MFB model). The sections show the lesion of ventral midbrain dopaminergic neurons and the brain areas studied. The sections were cut at ca. −3.2 mm from bregma, immunostained for tyrosine hydroxylase and imaged at 4x magnification. Delineation of the subdivisions of the substantia nigra pars compacta followed Fu et al. (2012) on all anterior-posterior levels.

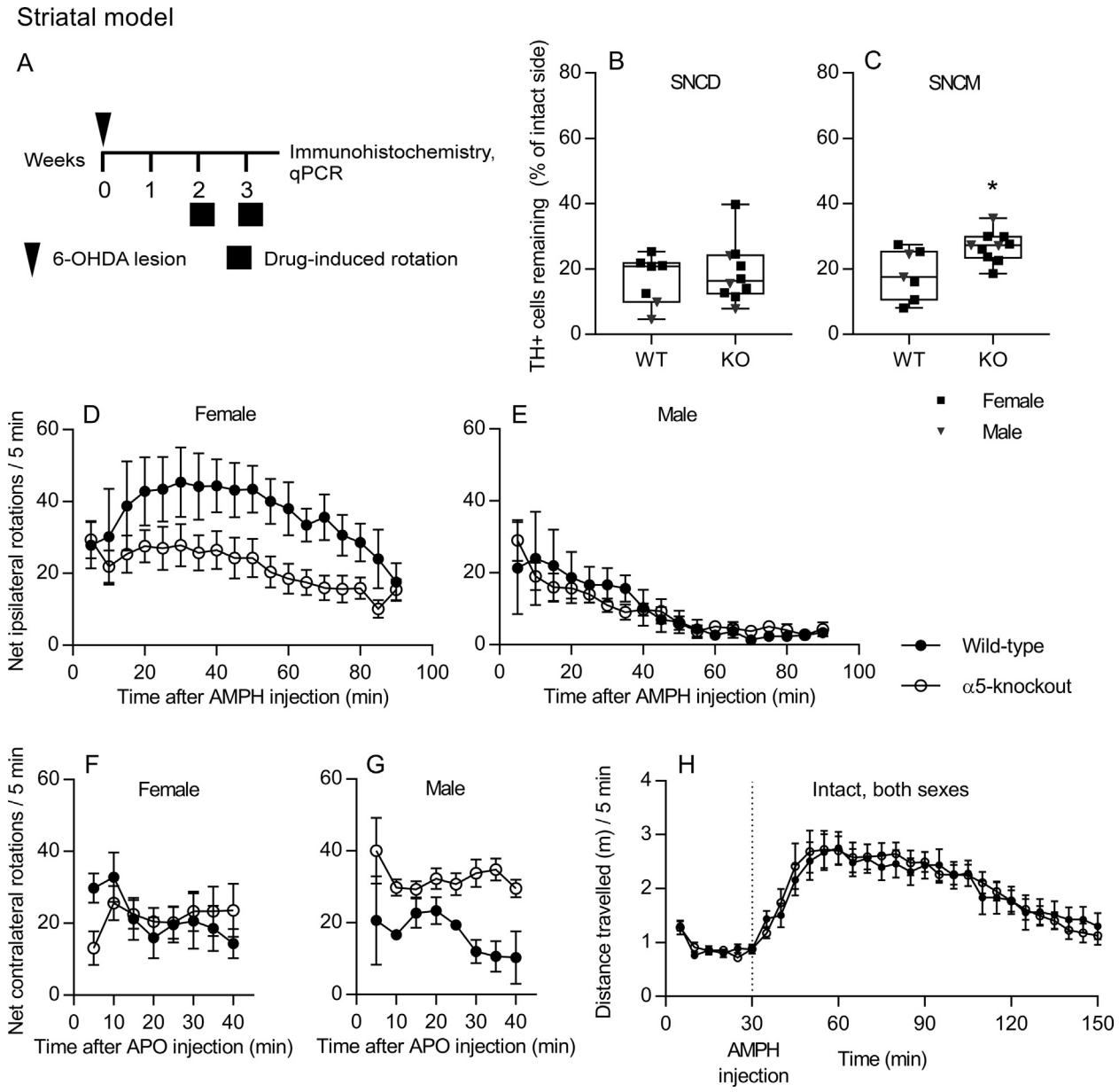

Fig. 2. Measures of dopaminergic denervation and motor dysfunction in intrastriatally lesioned mice. A: Experiment timeline. Mice were lesioned with 6-OHDA injections into the striatum. Amphetamine- and apomorphine-induced rotational behavior was assessed after recovery. Lesion extent was determined 30 days after the lesion and was found to be fairly severe in both the SNCD and the SNCM. B: In the SNCD, no genotype difference in lesion extent was observed, but the lesion tended to be more severe in male animals ($P = 0.065$, 2-way ANOVA; $n = 7$ WT, 10 KO; both sexes). C: The lesion in the SNCM was less severe in α5-KO mice than WT mice (*, $P < 0.05$, 2-way ANOVA; $n = 7$ WT, 10 KO; both sexes). D: Amphetamine (2.5 mg/kg) induced fewer rotations in female α5-KO mice when compared to female WT mice ($P < 0.05$, 2-way RM-ANOVA, $n = 5$ WT, 8 KO). E: No statistically significant genotype difference in amphetamine-induced rotations in male animals ($n = 3$ WT, 4 KO). F: Among female animals, contralateral rotational behavior after apomorphine (0.5 mg/kg) administration tended to be reduced in α5-KO mice at the beginning of the measurement (genotype × time interaction $P = 0.10$, 2-way RM-ANOVA, $n = 5$ WT, 8 KO). G: Among male animals, α5-KO mice performed more apomorphine-induced rotations ($P = 0.01$, 2-way RM-ANOVA, $n = 3$ WT, 4 KO). H: In intact animals, no genotype difference was observed in distance travelled after amphetamine (2.5 mg/kg) administration ($n = 13$ WT, 14 KO; both sexes). Immunohistochemical data (B–C) shown as box plots of median, quartiles, range and distribution for each genotype. Behavioral data (D–H) shown as mean ± SEM. 6-OHDA = 6-hydroxydopamine; SNCD = dorsal tier, SNCM = medial cluster of the substantia nigra pars compacta; AMPH = amphetamine; APO = apomorphine.

WT mice (Fig. 3D; main effect of genotype, $F(1,18) = 3.70$, $P = 0.070$). A similar observation was made in MFB-lesioned male mice in the pilot experiment (Figure S2).

3.2. Attenuated levodopa-induced dyskinesia and no antidyskinetic effect by nicotine in α5-KO mice

When mice lesioned with intra-MFB 6-OHDA injections were chronically administered levodopa and benserazide, α5-KO mice developed less severe levodopa-induced dyskinesia than WT mice (Fig. 3E; main effect of genotype, $F(1,14) = 12.3$, $P = 0.004$). In animals treated chronically with nicotine in saccharin-sweetened drinking water, dyskinesia severity decreased gradually over time in the case of WT but not α5-KO mice (genotype × treatment × time interaction, $F(3.5,48.5) = 3.14$, $P = 0.028$; genotype × time interaction in nicotine-treated animals, $F(3.2,22.3) = 4.73$, $P = 0.010$). The average daily intake of nicotine (calculated from drinking water consumption) at the highest

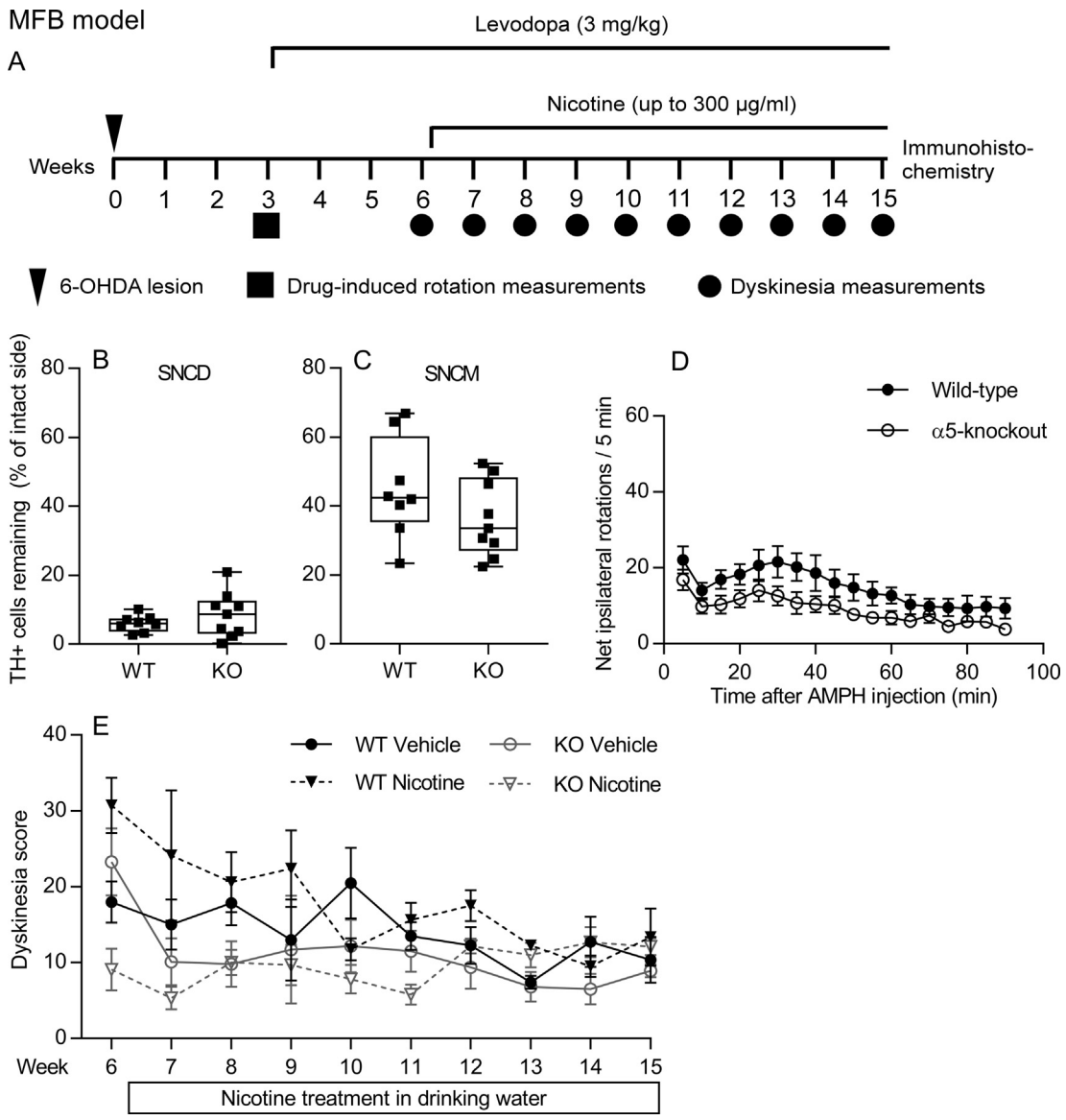

Fig. 3. Measures of dopaminergic denervation and motor dysfunction in intra-MFB lesioned mice. A: Experiment timeline. Mice were lesioned with intra-MFB 6-OHDA injections. Amphetamine-induced rotational behavior was assessed after recovery. Mice were then chronically administered (s.c.) levodopa (3 mg/kg) and benserazide (15 mg/kg) for 12 weeks and, simultaneously, either nicotine (p.o., up to 300 µg/ml) or vehicle (saccharin-sweetened drinking water) for 9 weeks. Lesion extent was determined 15 weeks after the lesion and found to be severe in the SNCD but partial in the SNCM. B–C: No statistically significant genotype differences in lesion extent were observed ($n = 8$ WT, 10 KO; all female). D: Amphetamine (2.5 mg/kg) tended to induce fewer ipsilateral rotations in α5-KO mice than WT mice ($P = 0.07$, 2-way RM-ANOVA, $n = 10$ per genotype; all female). E: α5-KO mice developed less severe levodopa-induced dyskinesia than WT mice ($P < 0.01$, 3-way RM-ANOVA, $n = 8$ WT, 10 KO; all female). In nicotine-treated mice, dyskinesia severity was reduced over time in WT but not α5-KO mice (genotype × treatment × time interaction, $P < 0.05$; genotype × time interaction in nicotine-treated animals, $P = 0.01$; $n = 4–5$ per group). Immunohistochemical data (B–C) shown as box plots of median, quartiles, range and distribution for each genotype. Behavioral data (D–E) shown as mean ± SEM. MFB = medial forebrain bundle; 6-OHDA = 6-hydroxydopamine; SNCD = dorsal tier, SNCM = medial cluster of the substantia nigra pars compacta; AMPH = amphetamine.

concentration of 300 µg/ml was 31 mg/kg.

3.3. *Effects of α5 gene deletion on dopamine uptake, dopamine transporter protein, dopamine tissue levels and dopamine receptor expression in the striatum*

Uptake of dopamine into striatal synaptosomes (Fig. 4A) was statistically significantly decreased in intact α5-KO mice, suggesting reduced dopamine transporter function (main effect of genotype, $F(1,22) = 6.62$, $P = 0.017$). Dopamine uptake was larger in male than female animals (main effect of sex, $F(1,22) = 6.30$, $P = 0.020$), but the genotype difference was similar in both sexes (genotype × sex interaction, $F(1,22) = 0.512$, $P = 0.482$).

Striatal DAT and pDAT protein levels were measured with Western blotting (Fig. 4B). No statistically significant genotype or sex differences were found (DAT: main effect of genotype, $F(1,10) = 1.05$, $P = 0.330$; main effect of sex, $F(1,10) = 0.37$, $P = 0.554$; genotype × sex interaction, $F(1,10) = 0.05$, $P = 0.821$; pDAT: main effect of genotype, $F(1,10) = 0.38$, $P = 0.551$; main effect of sex, $F(1,10) = 0.20$, $P = 0.667$; genotype × sex interaction, $F(1,10) = 3.74$, $P = 0.082$). See supplementary data (Figure S3) for images of all Western blots.

No statistically significant genotype or sex differences were found in striatal tissue concentrations of dopamine and its metabolites, measured with HPLC from intact mice (Fig. 4C; dopamine: main effect of genotype, $F(1,18) = 0.317$, $P = 0.581$; main effect of

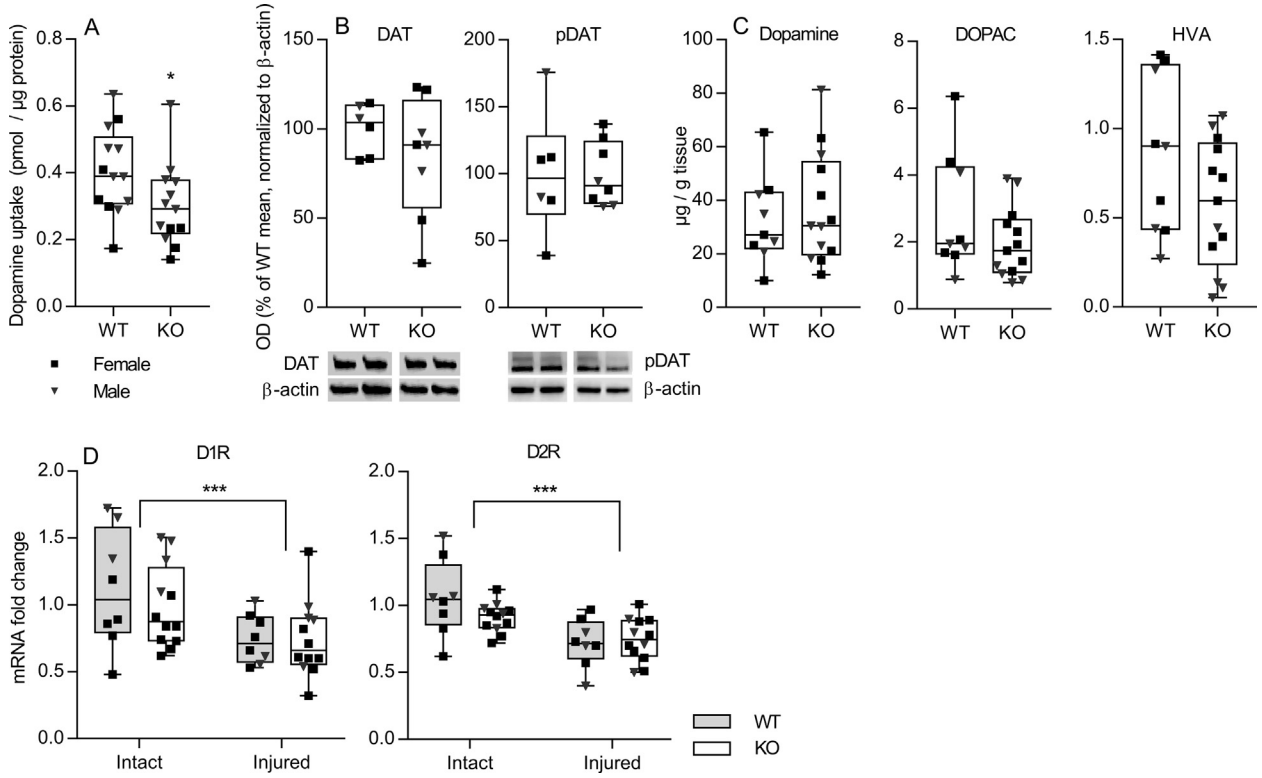

Fig. 4. Biomarkers of the dopaminergic system of α5-KO mice. A: Uptake of dopamine into striatal synaptosomes was decreased in intact α5-KO animals, suggesting reduced dopamine transporter function (*, $P < 0.05$, 2-way ANOVA; $n = 13$ animals per genotype assayed in triplicate; both sexes). In addition, dopamine uptake was larger in male than female animals ($P < 0.05$). B: No statistically significant genotype differences in striatal DAT or phospho (T53)-DAT protein expression in intact animals ($n = 6$ WT, 8 KO; both sexes). Two example Western blot images per genotype shown; see supplementary data for full images. C: No statistically significant genotype or sex differences in striatal tissue concentrations of dopamine and its metabolites as measured by high-performance liquid chromatography from intact animals ($n = 9$ WT, 13 KO; both sexes). D: Striatal expression of D1R and D2R mRNA in mice lesioned with intrastriatal 6-OHDA injections. Expression of both receptors' mRNA was decreased in the lesioned hemisphere (***, $P < 0.001$, 3-way ANOVA; $n = 8$ WT, 12 KO assayed in duplicate; both sexes) but similar in WT and α5-KO animals. In male animals, D1R mRNA expression was larger ($P < 0.001$) and more markedly decreased by the lesion (sex × hemisphere interaction, $P < 0.001$) when compared to female animals. In addition, tendencies were observed for a greater lesion-induced reduction of D2R mRNA expression in male animals (sex × hemisphere interaction, $P = 0.061$) and in wild-type animals (genotype × hemisphere interaction, $P = 0.098$). Plots show median, quartiles, range and distribution for each genotype (A–D) and hemisphere (D). DAT = dopamine transporter; pDAT = phospho (T53)-DAT; OD = optical density; DOPAC = 3,4-dihydroxyphenylacetic acid; HVA = homovanillic acid; D1R = dopamine 1 receptor; D2R = dopamine 2 receptor.

sex, $F(1,18) = 0.022$, $P = 0.884$; DOPAC: main effect of genotype, $F(1,18) = 1.45$, $P = 0.245$; main effect of sex, $F(1,18) = 0.742$, $P = 0.400$; HVA: main effect of genotype, $F(1,18) = 2.46$, $P = 0.134$; main effect of sex, $F(1,18) = 1.33$, $P = 0.263$). No significant genotype × sex interactions were found. No statistically significant genotype or sex differences in metabolite/dopamine ratios were found (data not shown).

The striatal expression of dopamine D1 and D2 receptor (D1R and D2R) mRNA (Fig. 4D) was measured with qPCR from intrastriatally lesioned mice. The dopaminergic lesion significantly reduced D1R mRNA expression (main effect of hemisphere, $F(1,32) = 25.9$, $P < 0.001$), but expression did not differ between genotypes (main effect of genotype, $F(1,32) = 0.476$, $P = 0.495$; genotype × hemisphere interaction, $F(1,32) = 0.952$, $P = 0.337$). D1R mRNA expression was significantly larger in male than female animals (main effect of sex, $F(1,32) = 21.2$, $P < 0.001$) and, furthermore, was more markedly decreased by the lesion in male animals (sex × hemisphere interaction, $F(1,32) = 14.6$, $P < 0.001$). Similarly, the dopaminergic lesion significantly reduced D2R mRNA expression (main effect of hemisphere, $F(1,32) = 21.2$, $P < 0.001$) with the expression not differing between genotypes (main effect of genotype, $F(1,32) = 1.21$, $P = 0.280$). In contrast to D1R mRNA, D2R mRNA expression was not larger in male animals (main effect of sex, $F(1,32) = 0.283$, $P = 0.598$). However, similar to D1R mRNA, D2R mRNA expression in males tended to be more markedly decreased by the lesion (sex × hemisphere interaction, $F(1,32) = 3.77$, $P = 0.061$). In addition, a tendency was observed for a greater lesion-induced decrease of D2R mRNA in wild-type than α5-KO animals (genotype × hemisphere interaction, $F(1,32) = 2.91$, $P = 0.098$).

4. Discussion

Nicotinic acetylcholine receptors show promise as drug targets for Parkinson's disease (Quik et al., 2015). Here, we studied the effects of α5 nicotinic receptor subunit deletion in mouse models of Parkinson's disease and levodopa-induced dyskinesia. Taken together, the results suggest that the lack of α5* receptors resulted in attenuation of the hemiparkinsonian neurodegeneration and motor dysfunction induced by unilateral neurotoxic lesioning of the nigrostriatal dopaminergic pathway. The study represents the first characterization of the role of α5* nicotinic receptors in Parkinson's disease, and raises intriguing possibilities for their use as a target in the disease's treatment.

The main finding of the study is that the death of dopaminergic neurons induced by intrastriatal injections of 6-OHDA was attenuated in α5-KO mice, specifically within the medial cluster of the SNC (SNCM). This neuroprotective effect by α5-KO was paralleled by attenuation of amphetamine-induced rotation, a widely-used test where rotational behavior relates to the degree of

dopaminergic denervation (Bové and Perier, 2012). Although it should be noted that attenuated rotational behavior was not observed in male intrastriatally lesioned animals (see below for further discussion on this sex difference), the behavioral finding suggests that the neuroprotective effect in the SNCM was significant enough to result in attenuated hemiparkinsonian motor dysfunction. Importantly, no genotype difference in locomotor activity was found after amphetamine administration in intact animals, further suggesting that the observed attenuation of rotational behavior was linked to the lessened neurodegeneration. Interestingly, the present finding of attenuated amphetamine-induced ipsilateral circling associated with less severe lesioning of the SNCM is in line with a previous study, utilizing electrically lesioned rats, where damage to the medial but not the lateral substantia nigra resulted in ipsilateral circling in response to amphetamine (Vaccarino and Franklin, 1982).

In female animals lesioned utilizing intra-MFB 6-OHDA injections, lesion extent in the SNC did not differ between wild-type and α5-KO mice. Nevertheless, attenuated dopaminergic motor dysfunction was observed also in α5-KO animals of the MFB model, as evidenced by a tendency for attenuated amphetamine-induced rotation as well as less severe levodopa-induced dyskinesia. The contrasting SNC immunohistochemical results from the two experiments utilizing different lesion models could be explained by their different time courses. In the experiments utilizing the intrastriatal model, lesion extent was assessed 1–2 weeks after the rotametry experiments, capturing the state of the midbrain soon after the behavioral assays. In contrast, in the experiments utilizing the intra-MFB model, several months of chronic treatment with levodopa, benserazide and either nicotine or vehicle interceded between the rotametry measurements and immunohistochemistry. Possible confounding phenomena include neuroprotective (Quik et al., 2015) or other effects of nicotine, effects of levodopa – able to induce a TH-positive phenotype in at least striatal neurons (Darmopil et al., 2008; Francardo et al., 2011) – or even spontaneous neuronal recovery, reported in 6-OHDA-lesioned mice at least in the striatum (Bez et al., 2016). Alternatively, it is possible that the more severe dopaminergic neurotoxicity induced in the MFB model (see e.g., Bové and Perier, 2012) resulted in the masking of any protective effect by α5-KO.

The observed neuroprotective consequences of α5 subunit deletion may be linked to the reduced DAT function (manifesting as reduced dopamine uptake) observed in intact α5-KO animals. As 6-OHDA is taken up via the DAT (Simola et al., 2007), the reduced DAT function may have led to reduced 6-OHDA uptake into dopaminergic neurons and therefore to attenuated dopaminergic neurotoxicity. Notably, nicotinic receptor activation has previously been found to increase dopamine clearance and DAT cell surface expression (Middleton et al., 2004; Zhu et al., 2009), showing that nicotinic signaling can indeed modulate DAT function. In the present study, the reduced dopamine uptake observed in α5-KO animals appeared to be purely a case of reduced DAT activity, as no genotype difference in striatal DAT protein levels was found. As DAT activity and membrane expression is regulated by phosphorylation (Vaughan et al., 1997; Morón et al., 2003), with major involvement in activity modulation by the phosphorylation site T53 (Foster et al., 2012), we also measured the striatal levels of phospho (T53)-DAT. No genotype difference was observed in pDAT levels, suggesting that the decreased activity was mediated by other mechanisms than changes in DAT T53 phosphorylation.

Another possible explanation for the attenuated dopaminergic denervation is reduced calcium influx and consequently reduced oxidative stress in animals lacking α5* receptors. Incorporation of the α5 subunit to a nicotinic receptor results in increased calcium permeability (Tapia et al., 2007), and α5* receptors have a crucial role in nicotinic receptor-mediated calcium fluxes in at least some dopaminergic neurons of the ventral midbrain (Sciaccaluga et al., 2015). On the other hand, the neurotoxic effects of 6-OHDA are suggested to be caused by oxidative stress (Simola et al., 2007) and amplified by cytoplasmic free calcium (Blum et al., 2001), with increased striatal intracellular calcium concentrations found in 6-OHDA-treated rats (Kumar et al., 1995). Interestingly, cytosolic reactive oxygen species are able to inactivate nicotinic receptors, possibly as a protective mechanism against excess calcium influx (Campanucci et al., 2008; Krishnaswamy and Cooper, 2012).

It is unclear why a neuroprotective effect mediated by either reduced DAT function or reduced calcium influx would manifest specifically in neurons of the SNCM. It may be of relevance that when compared to dopamine neurons of the dorsal tier of the SNC (SNCD), a much higher proportion of dopamine neurons in the mouse SNCM express the calcium-binding protein calbindin (Fu et al., 2012), suggesting that they may be more resistant to calcium-linked toxicity. On the other hand, no difference in DAT expression was found between mouse SNCD and SNCM dopamine neurons (Fu et al., 2012). To the best of our knowledge it remains to be determined whether dopamine neurons of the different mouse SNC regions differ in other aspects of calcium signaling or their expression of α5* receptors.

If the attenuated dopaminergic neurodegeneration in α5*-lacking animals after a 6-OHDA insult translates to a more general neuroprotective effect, the present results could represent a significant finding in the field of dopaminergic neuroprotection, suggesting potential for α5* receptor disruption as a novel avenue for treatment of Parkinson's disease. Importantly, both the dopamine transporter (Storch et al., 2004) and calcium-linked oxidative stress (Chan et al., 2009; Surmeier, 2007) have been suggested to be of major importance in the pathophysiology of human Parkinson's disease, particularly related to the selective vulnerability of SNC dopaminergic neurons. However, the possibility that the observed neuroprotective effect is specific to the 6-OHDA neurotoxin model must also be acknowledged. This may be true particularly if the attenuated neurodegeneration was indeed the result of reduced DAT function and diminished 6-OHDA uptake. Future studies could shed light on this question by investigating the effects of α5 gene deletion in other neurotoxin or genetic models of Parkinson's disease. Further studies could also investigate the contribution of α5* receptors to the established neuroprotective effects of nicotinic drugs (Quik et al., 2015).

Interestingly, while dopaminergic denervation in the MFB lesion model is typically more severe than in the striatal model (Bové and Perier, 2012), and indeed in the present study was more severe in the SNCD, cell loss in the SNCM was less severe in the MFB model. This suggests that spontaneous or drug-induced recovery may indeed have occurred and perhaps been more pronounced within the SNCM. Alternatively, the relatively well-spared SNCM could be due to a presence of projections from the SNCM to the dorsal striatum that do not pass through the MFB coordinates where 6-OHDA was injected.

Besides the main finding of lessened dopaminergic denervation in the SNCM, the attenuated rotational behavior observed in lesioned α5-KO animals after amphetamine administration could in part also be related to their reduced DAT function. Pointing to this possibility is amphetamine's mechanism of action, which depends greatly on the DAT (Fleckenstein et al., 2007). However, as mentioned above intact α5-KO animals did not show attenuated or otherwise changed locomotor activity after amphetamine administration. This suggests that the attenuated rotational behavior in lesioned animals was not due to reduced responsiveness to amphetamine. It is possible in principle, however, that the reduced DAT function had behavioral consequences which only surfaced in

conditions of dopaminergic denervation.

Surprisingly, male mice lesioned with intrastriatal 6-OHDA injections exhibited a contrasting pattern of genotype differences in rotational behavior. As no significant sex or genotype differences were found in intact animals' motor response to amphetamine, and in the MFB model both male and female α5-KO mice showed attenuation of amphetamine-induced rotation (see supplementary data), this sex difference appears to be linked specifically to the intrastriatal 6-OHDA model. While little is known about possible sex differences related to α5* receptors, the female sex hormone progesterone has been shown to upregulate α5* expression (Gangitano et al., 2009). The lack of significant attenuation of rotational behavior in response to α5 deletion in male mice could therefore have been the result of lower α5* receptor expression already in wild-type animals. Furthermore, the lack of a similar sex difference in the MFB model could be related to the near-total loss of striatal α5-expressing dopamine terminals characteristic for intra-MFB 6-OHDA injections.

The contrasting behavioral findings in intrastriatally lesioned male mice could also be related to the sex differences observed in some biomarkers of the dopaminergic system. More efficient dopamine uptake in male mice could in principle explain the somewhat shorter duration of amphetamine's effects seen in intrastriatally lesioned male animals, although no such sex difference was observed in intact or MFB-lesioned animals. Finally, a relatively larger lesion-induced loss of D1 and possibly D2 receptor mRNA was observed in the intrastriatally lesioned male animals when compared to female animals, and may in part underlie the divergent behavioral findings.

In the present study, we also observed attenuated levodopa-induced dyskinesia in mice lacking the α5* receptor. Attenuated dyskinesia could be explained by less severe denervation (Francardo et al., 2011; Lundblad et al., 2004). However, no genotype difference in lesion extent was observed in the experiment in question (MFB model). Thus, the attenuated dyskinesia in α5-KO animals may also have been the result of some as of yet unestablished mechanism, perhaps analogous to similar findings in mice lacking the α6 nicotinic receptor subunit (Quik et al., 2012) or related to the decreased DAT function. In addition, when dyskinetic mice were chronically treated with nicotine, dyskinesia severity was gradually reduced in wild-type animals but not in α5-KO animals. This suggests that similar to other β2* nicotinic receptors (Quik et al., 2015), α5-containing nicotinic receptors may be involved in nicotine's antidyskinetic effects and a potential target for more selective antidyskinetic treatments.

In conclusion, our observations in hemiparkinsonian mice suggest that the lack of α5* nicotinic receptors results in attenuated dopaminergic neurodegeneration and motor dysfunction in a 6-OHDA neurotoxin model of Parkinson's disease. The findings raise the possibility of utilizing α5* nicotinic receptors as a novel drug target in the treatment of Parkinson's disease and LID, and expand the sum of evidence suggesting that various nicotinic receptor subtypes are crucially involved in the pathophysiology of the disease. Future studies on the effects of α5 subunit disruption in animal models of neurodegenerative disorders are warranted and necessary to obtain more evidence of the mechanisms behind these findings.

Authorship contributions

OS managed the research project. SL, SKK, SR and OS planned the studies. SL, SKK, RH and TT performed data acquisition. All authors participated in data analysis and interpretation. SL wrote the manuscript, and all other authors participated in its review and approved the final version.

Funding sources

This work was supported by the Academy of Finland (grant number 12677612); the Finnish Parkinson Foundation; and the Finnish Pharmaceutical Society.

Declarations of interest

None.

Acknowledgments

The authors would like to thank Dr. Michael J. Marks (University of Colorado) for the α5-KO animals, Dr. Timo Myöhänen for access to his Western blotting equipment and expertise, Ulrika Julku and Reinis Svarcbahs for technical advice, and Sara Figuerola Santamonica, Kati Rautio, Laura Benning and Veeti Vornanen for their help in data acquisition.

Appendix A. Supplementary data

Supplementary data related to this article can be found at https://doi.org/10.1016/j.neuropharm.2018.06.028.

References

Albuquerque, E.X., Pereira, E.F.R., Alkondon, M., Rogers, S.W., 2009. Mammalian nicotinic acetylcholine receptors: from structure to function. Physiol. Rev. 89, 73–120. https://doi.org/10.1152/physrev.00015.2008.

Bailey, C.D.C., De Biasi, M., Fletcher, P.J., Lambe, E.K., 2010. The nicotinic acetylcholine receptor α5 subunit plays a key role in attention circuitry and accuracy. J. Neurosci. 30, 9241–9252. https://doi.org/10.1523/JNEUROSCI.2258-10.2010.

Bastide, M.F., Meissner, W.G., Picconi, B., Fasano, S., Fernagut, P.O., Feyder, M., Francardo, V., Alcacer, C., Ding, Y., Brambilla, R., Fisone, G., Jon Stoessl, A., Bourdenx, M., Engeln, M., Navailles, S., De Deurwaerdère, P., Ko, W.K.D., Simola, N., Morelli, M., Groc, L., Rodriguez, M.C., Gurevich, E.V., Quik, M., Morari, M., Mellone, M., Gardoni, F., Tronci, E., Guehl, D., Tison, F., Crossman, A.R., Kang, U.J., Steece-Collier, K., Fox, S., Carta, M., Angela Cenci, M., Bézard, E., 2015. Pathophysiology of L-dopa-induced motor and non-motor complications in Parkinson's disease. Prog. Neurobiol. 132, 96–168. https://doi.org/10.1016/j.pneurobio.2015.07.002.

Besson, M., Guiducci, S., Granon, S., Guilloux, J.P., Guiard, B., Repérant, C., Faure, P., Pons, S., Cannazza, G., Zoli, M., Gardier, A.M., Maskos, U., 2016. Alterations in alpha5* nicotinic acetylcholine receptors result in midbrain- and hippocampus-dependent behavioural and neural impairments. Psychopharmacology (Berlin) 233, 3297–3314. https://doi.org/10.1007/s00213-016-4362-2.

Bez, F., Francardo, V., Cenci, M.A., 2016. Dramatic differences in susceptibility to L-DOPA-induced dyskinesia between mice that are aged before or after a nigrostriatal dopamine lesion. Neurobiol. Dis. 94, 213–225. https://doi.org/10.1016/j.nbd.2016.06.005.

Blum, D., Torch, S., Lambeng, N., Nissou, M.F., Benabid, A.L., Sadoul, R., Verna, J.M., 2001. Molecular pathways involved in the neurotoxicity of 6-OHDA, dopamine and MPTP: contribution to the apoptotic theory in Parkinson's disease. Prog. Neurobiol. 65, 135–172. https://doi.org/10.1016/S0301-0082(01)00003-X.

Bordia, T., McGregor, M., Papke, R.L., Decker, M.W., McIntosh, J.M., Quik, M., 2015. The α7 nicotinic receptor agonist ABT-107 protects against nigrostriatal damage in rats with unilateral 6-hydroxydopamine lesions. Exp. Neurol. 263, 277–284. https://doi.org/10.1016/j.expneurol.2014.09.015.

Bové, J., Perier, C., 2012. Neurotoxin-based models of Parkinson's disease. Neuroscience 211, 51–76. https://doi.org/10.1016/j.neuroscience.2011.10.057.

Chan, C.S., Gertler, T.S., Surmeier, J.D., 2009. Calcium homeostasis, selective vulnerability and Parkinson's disease. Trends Neurosci. 32, 249–256. https://doi.org/10.1016/j.tins.2009.01.006.

Campanucci, A., Krishnaswamy, A., Cooper, E., 2008. Mitochondrial reactive oxygen species inactivate neuronal nicotinic acetylcholine receptors and induce long-term depression of fast nicotinic synaptic transmission. J. Neurosci. 28, 1733–1744. https://doi.org/10.1523/JNEUROSCI.5130-07.2008.

Darmopil, S., Muñetón-Gómez, V.C., De Ceballos, M.L., Bernson, M., Moratalla, R., 2008. Tyrosine hydroxylase cells appearing in the mouse striatum after dopamine denervation are likely to be projection neurones regulated by L-DOPA. Eur. J. Neurosci. 27, 580–592. https://doi.org/10.1111/j.1460-9568.2008.06040.x.

Dauer, W., Przedborski, S., 2003. Parkinson's disease: mechanisms and models. Neuron 39, 889–909. https://doi.org/10.1016/S0896-6273(03)00568-3.

Exley, R., McIntosh, J.M., Marks, M.J., Maskos, U., Cragg, S.J., 2012. Striatal α5 nicotinic receptor subunit regulates dopamine transmission in dorsal striatum. J. Neurosci. 32, 2352–2356. https://doi.org/10.1523/JNEUROSCI.4985-11.2012.

Fleckenstein, A.E., Volz, T.J., Riddle, E.L., Gibb, J.W., Hanson, G.R., 2007. New insights

into the mechanism of action of amphetamines. Annu. Rev. Pharmacol. Toxicol. 47, 681–698. https://doi.org/10.1146/annurev.pharmtox.47.120505.105140.
Foster, J.D., Yang, J., Moritz, A.E., ChallaSivaKanaka, S., Smith, M.A., Holy, M., Wilebski, K., Sitte, H.H., Vaughan, R.A., 2012. Dopamine transporter phosphorylation site Threonine 53 regulates substrate reuptake and amphetamine-stimulated efflux. J. Biol. Chem. 287, 29702–29712. https://doi.org/10.1074/jbc.M112.367706.
Francardo, V., Recchia, A., Popovic, N., Andersson, D., Nissbrandt, H., Cenci, M.A., 2011. Impact of the lesion procedure on the profiles of motor impairment and molecular responsiveness to L-DOPA in the 6-hydroxydopamine mouse model of Parkinson's disease. Neurobiol. Dis. 42, 327–340. https://doi.org/10.1016/j.nbd.2011.01.024.
Franklin, K.B.J., Paxinos, G., 1997. The Mouse Brain in Stereotaxic Coordinates. Academic Press, San Diego.
Fu, Y.H., Yuan, Y., Halliday, G., Rusznák, Z., Watson, C., Paxinos, G., 2012. A cytoarchitectonic and chemoarchitectonic analysis of the dopamine cell groups in the substantia nigra, ventral tegmental area, and retrorubral field in the mouse. Brain Struct. Funct. 217, 591–612. https://doi.org/10.1007/s00429-011-0349-2.
Gangitano, D., Salas, R., Teng, Y., Perez, E., De Biasi, M., 2009. Progesterone modulation of α5 nAChR subunits influences anxiety-related behavior during estrus cycle. Genes Brain Behav. 8, 398–406. https://doi.org/10.1111/j.1601-183X.2009.00476.x.
Grady, S.R., Wageman, C.R., Patzlaff, N.E., Marks, M.J., 2012. Low concentrations of nicotine differentially desensitize nicotinic acetylcholine receptors that include α5 or α6 subunits and that mediate synaptosomal neurotransmitter release. Neuropharmacology 62, 1935–1943. https://doi.org/10.1016/j.neuropharm.2011.12.026.
Gundersen, H.J.G., Bagger, P., Bendtsen, T.F., Evans, S.M., Korbo, L., Marcussen, N., Møller, A., Nielsen, K., Nyengaard, J.R., Pakkenberg, B., Sørensen, F.B., Vesterby, A., West, M.J., 1988. The new stereological tools: disector, fractionator, nucleator and point sampled intercepts and their use in pathological research and diagnosis. APMIS 96, 857–881. https://doi.org/10.1111/j.1699-0463.1988.tb00954.x.
Huang, L.Z., Grady, S.R., Quik, M., 2011. Nicotine reduces L-DOPA-induced dyskinesias by acting at β2* nicotinic receptors. J. Pharmacol. Exp. Therapeut. 338, 932–941. https://doi.org/10.1124/jpet.111.182949.
Jackson, K.J., Marks, M.J., Vann, R.E., Chen, X., Gamage, T.F., Warner, J.A., Damaj, M.I., 2010. Role of α5 nicotinic acetylcholine receptors in pharmacological and behavioral effects of nicotine in mice. J. Pharmacol. Exp. Therapeut. 334, 137–146. https://doi.org/10.1124/jpet.110.165738.
Julku, U.H., Panhelainen, A.E., Tiilikainen, S.E., Svarcbahs, R., Tammimäki, A.E., Piepponen, T.P., Savolainen, M.H., Myöhänen, T.T., 2018. Prolyl oligopeptidase regulates dopamine transporter phosphorylation in the nigrostriatal pathway of mouse. Mol. Neurobiol. 55, 470–482. https://doi.org/10.1007/s12035-016-0339-8.
Krishnaswamy, A., Cooper, E., 2012. Reactive oxygen species inactivate neuronal nicotinic acetylcholine receptors through a highly conserved cysteine near the intracellular mouth of the channel: implications for diseases that involve oxidative stress. J. Physiol. 590, 39–47. https://doi.org/10.1113/jphysiol.2011.214007.
Kumar, R., Agarwal, A.K., Seth, P.K., 1995. Free radical-generated neurotoxicity of 6-hydroxydopamine. J. Neurochem. 64, 1703–1707. https://doi.org/10.1046/j.1471-4159.1995.64041703.x.
Kuryatov, A., Onksen, J., Lindstrom, J., 2008. Roles of accessory subunits in α4β2* nicotinic receptors. Mol. Pharmacol. 74, 132–143. https://doi.org/10.1124/mol.108.046789.
Leino, S., Koski, S.K., Rannanpää, S., Salminen, O., 2018. Effects of antidyskinetic nicotine treatment on dopamine release in dorsal and ventral striatum. Neurosci. Lett. 672, 40–45. https://doi.org/10.1016/j.neulet.2018.02.042.
Livak, K.J., Schmittgen, T.D., 2001. Analysis of relative gene expression data using real-time quantitative PCR and the $2^{-\Delta\Delta CT}$ method. Methods 25, 402–408. https://doi.org/10.1006/meth.2001.1262.
Livingstone, P.D., Wonnacott, S., 2009. Nicotinic acetylcholine receptors and the ascending dopamine pathways. Biochem. Pharmacol. 78, 744–755. https://doi.org/10.1016/j.bcp.2009.06.004.
Lundblad, M., Picconi, B., Lindgren, H., Cenci, M.A., 2004. A model of L-DOPA-induced dyskinesia in 6-hydroxydopamine lesioned mice: relation to motor and cellular parameters of nigrostriatal function. Neurobiol. Dis. 16, 110–123. https://doi.org/10.1016/j.nbd.2004.01.007.
Middleton, L.S., Cass, W.A., Dwoskin, L.P., 2004. Nicotinic receptor modulation of dopamine transporter function in rat striatum and medial prefrontal cortex. J. Pharmacol. Exp. Therapeut. 308, 367–377. https://doi.org/10.1124/jpet.103.055335.
Mijatovic, J., Airavaara, M., Planken, A., Auvinen, P., Raasmaja, A., Piepponen, T.P., Costantini, F., Ahtee, L., Saarma, M., 2007. Constitutive Ret activity in knock-in multiple endocrine neoplasia type B mice induces profound elevation of brain dopamine concentration via enhanced synthesis and increases the number of TH-positive cells in the substantia nigra. J. Neurosci. 27, 4799–4809. https://doi.org/10.1523/JNEUROSCI.5647-06.2007.
Millar, N.S., Gotti, C., 2009. Diversity of vertebrate nicotinic acetylcholine receptors. Neuropharmacology 56, 237–246. https://doi.org/10.1016/j.neuropharm.2008.07.041.
Morón, J.A., Zakharova, I., Ferrer, J.V., Merrill, G.A., Hope, B., Lafer, E.M., Lin, Z.C., Wang, J.B., Javitch, J.A., Galli, A., Shippenberg, T.S., 2003. Mitogen-activated protein kinase regulates dopamine transporter surface expression and dopamine transport capacity. J. Neurosci. 23, 8480–8488. https://doi.org/10.1523/JNEUROSCI.23-24-08480.2003.
Pietilä, K., Ahtee, L., 2000. Chronic nicotine administration in the drinking water affects the striatal dopamine in mice. Pharmacol. Biochem. Behav. 66, 95–103. https://doi.org/10.1016/S0091-3057(00)00235-5.
Quik, M., Bordia, T., Zhang, D., Perez, X.A., 2015. Nicotine and nicotinic receptor drugs: potential for Parkinson's disease and drug-induced movement disorders. Int. Rev. Neurobiol. 124, 247–271. https://doi.org/10.1016/bs.irn.2015.07.005.
Quik, M., Campos, C., Grady, S.R., 2013. Multiple CNS nicotinic receptors mediate L-dopa-induced dyskinesias: studies with parkinsonian nicotinic receptor knockout mice. Biochem. Pharmacol. 86, 1153–1162. https://doi.org/10.1016/j.bcp.2013.06.027.
Quik, M., Park, K.M., Hrachova, M., Mallela, A., Huang, L.Z., McIntosh, J.M., Grady, S.R., 2012. Role for α6 nicotinic receptors in L-dopa-induced dyskinesias in parkinsonian mice. Neuropharmacology 63, 450–459. https://doi.org/10.1016/j.neuropharm.2012.04.029.
Quik, M., Wonnacott, S., 2011. α6β2* and α4β2* nicotinic acetylcholine receptors as drug targets for Parkinson's disease. Pharmacol. Rev. 63, 938–966. https://doi.org/10.1124/pr.110.003269.
Ryan, R.E., Ross, S.A., Drago, J., Loiacono, R.E., 2001. Dose-related neuroprotective effects of chronic nicotine in 6-hydroxydopamine treated rats, and loss of neuroprotection in aα nicotinic receptor subunit knockout mice. Br. J. Pharmacol. 132, 1650–1656. https://doi.org/10.1038/sj.bjp.0703989.
Salas, R., Orr-Urtreger, A., Broide, R.S., Beaudet, A., Paylor, R., De Biasi, M., 2003. The nicotinic acetylcholine receptor subunit α5 mediates short-term effects of nicotine in vivo. Mol. Pharmacol. 63, 1059–1066. https://doi.org/10.1124/mol.63.5.1059.
Salminen, O., Murphy, K.L., McIntosh, J.M., Drago, J., Marks, M.J., Collins, A.C., Grady, S.R., 2004. Subunit composition and pharmacology of two classes of striatal presynaptic nicotinic acetylcholine receptors mediating dopamine release in mice. Mol. Pharmacol. 65, 1526–1535. https://doi.org/10.1124/mol.65.6.1526.
Schapira, A.H.V., Emre, M., Jenner, P., Poewe, W., 2009. Levodopa in the treatment of Parkinson's disease. Eur. J. Neurol. 16, 982–989. https://doi.org/10.1111/j.1468-1331.2009.02697.x.
Sciaccaluga, M., Moriconi, C., Martinello, K., Catalano, M., Bermudez, I., Stitzel, J.A., Maskos, U., Fucile, S., 2015. Crucial role of nicotinic α5 subunit variants for Ca^{2+} fluxes in ventral midbrain neurons. Faseb. J. 29, 3389–3398. https://doi.org/10.1096/fj.14-268102.
Simola, N., Morelli, M., Carta, A.R., 2007. The 6-hydroxydopamine model of Parkinson's disease. Neurotox. Res. 11, 151–167. https://doi.org/10.1007/BF03033565.
Storch, A., Ludolph, A.C., Schwarz, J., 2004. Dopamine transporter: involvement in selective dopaminergic neurotoxicity and degeneration. J. Neural. Transm. 111, 1267–1286. https://doi.org/10.1007/s00702-004-0203-2.
Surmeier, D.J., 2007. Calcium, ageing, and neuronal vulnerability in Parkinson's disease. Lancet Neurol. 6, 933–938. https://doi.org/10.1016/S1474-4422(07)70246-6.
Tapia, L., Kuryatov, A., Lindstrom, J., 2007. Ca^{2+} permeability of the $(\alpha4)_3(\beta2)_2$ stoichiometry greatly exceeds that of $(\alpha4)_2(\beta2)_3$ human acetylcholine receptors. Mol. Pharmacol. 71, 769–776. https://doi.org/10.1124/mol.106.030445.
Thiele, S.L., Warre, R., Khademullah, C.S., Fahana, N., Lo, C., Lam, D., Talwar, S., Johnston, T.H., Brotchie, J.M., Nash, J.E., 2011. Generation of a model of L-DOPA-induced dyskinesia in two different mouse strains. J. Neurosci. Meth. 197, 193–208. https://doi.org/10.1016/j.jneumeth.2011.02.012.
Tukey, J.W., 1977. Exploratory Data Analysis. Addison-Wesley, Reading.
Vaccarino, F., Franklin, K.B.J., 1982. Self-stimulation and circling reveal functional differences between medial and lateral substantia nigra. Behav. Brain Res. 5, 281–295. https://doi.org/10.1016/0166-4328(82)90034-1.
Vaughan, R.A., Huff, R.A., Uhl, G.R., Kuhar, M.J., 1997. Protein kinase C-mediated phosphorylation and functional regulation of dopamine transporters in striatal synaptosomes. J. Biol. Chem. 272, 15541–15546. https://doi.org/10.1074/jbc.272.24.15541.
Zhu, J., Apparsundaram, S., Dwoskin, L.P., 2009. Nicotinic receptor activation increases [^{3}H]dopamine uptake and cell surface expression of dopamine transporters in rat prefrontal cortex. J. Pharmacol. Exp. Therapeut. 328, 931–939. https://doi.org/10.1124/jpet.108.147025.